

The following resources related to this article are available online at www.sciencemag.org (this information is current as of December 9, 2009):

Updated information and services, including high-resolution figures, can be found in the online version of this article at:

<http://www.sciencemag.org/cgi/content/full/312/5772/440>

Supporting Online Material can be found at:

<http://www.sciencemag.org/cgi/content/full/312/5772/440/DC1>

This article **cites 26 articles**, 11 of which can be accessed for free:

<http://www.sciencemag.org/cgi/content/full/312/5772/440#otherarticles>

This article has been **cited by** 38 article(s) on the ISI Web of Science.

This article has been **cited by** 17 articles hosted by HighWire Press; see:

<http://www.sciencemag.org/cgi/content/full/312/5772/440#otherarticles>

Information about obtaining **reprints** of this article or about obtaining **permission to reproduce this article** in whole or in part can be found at:

<http://www.sciencemag.org/about/permissions.dtl>

Nuclear Pores Form de Novo from Both Sides of the Nuclear Envelope

Maximiliano A. D'Angelo,* Daniel J. Anderson,* Erin Richard, Martin W. Hetzert†

Nuclear pore complexes are multiprotein channels that span the double lipid bilayer of the nuclear envelope. How new pores are inserted into the intact nuclear envelope of proliferating and differentiating eukaryotic cells is unknown. We found that the Nup107-160 complex was incorporated into assembly sites in the nuclear envelope from both the nucleoplasmic and the cytoplasmic sides. Nuclear pore insertion required the generation of Ran guanosine triphosphate in the nuclear and cytoplasmic compartments. Newly formed nuclear pore complexes did not contain structural components of preexisting pores, suggesting that they can form de novo.

Nuclear pore complexes (NPCs) are the exclusive sites of trafficking between the nucleus and the cytoplasm (1, 2), and their biogenesis is crucial for the differentiation and metabolic activity of eukaryotic cells (3). In proliferating cells, the number of pores doubles during interphase before mitosis (4, 5). It is unclear whether NPC assembly occurs from the nucleoplasmic and/or cytoplasmic side(s) of the

nuclear envelope (NE) (6). It is also unknown whether existing NPCs serve as templates for new pores or whether NPCs assemble de novo (7–9).

To distinguish between these possibilities, we analyzed NPC assembly into intact NEs in vitro and in vivo. First, we established a cell-free NPC insertion assay using *Xenopus* egg extracts (10). We preassembled nuclei (NE-0) by incubating sperm chromatin and cytosol together

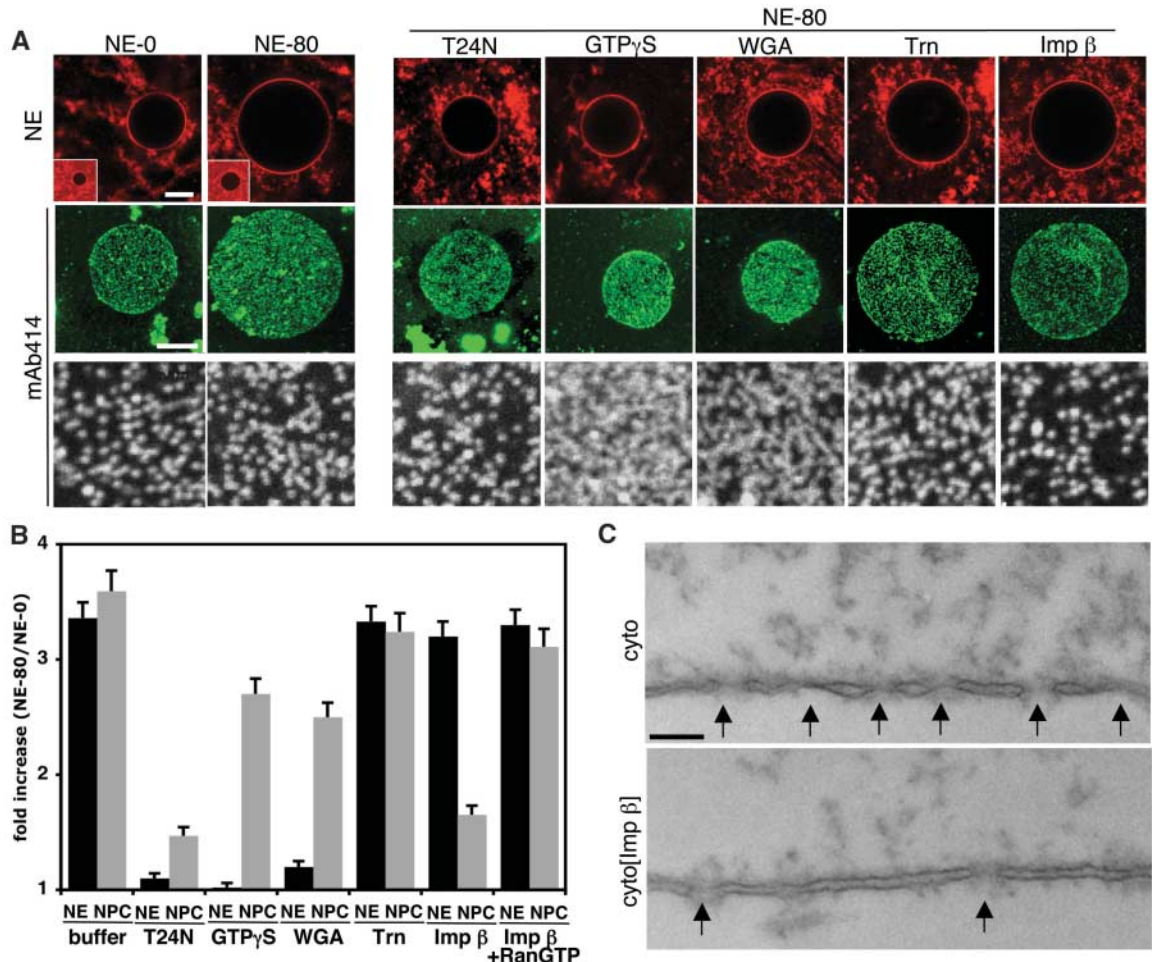
with fluorescently labeled membranes (11). NE-0 nuclei were incubated for an additional period of 80 min (NE-80), during which growth and NE expansion occurred (Fig. 1A). Both NE-0 and NE-80 nuclei were intact and excluded 70-kD dextran (Fig. 1A). NPCs were monitored with monoclonal antibody mAb414, which recognizes four nucleoporins (Fig. 1A) (12). During nuclear growth, the density of NPCs remained constant at 4.9 ± 0.6 NPCs/ μm^2 , indicating that new NPCs had been inserted into the expanding NE.

Using three-dimensional (3D) reconstructions of entire nuclei and visualization of individual NPCs by immunofluorescence (fig. S1, A to C), we found that the NE expanded from $920 \pm 104 \mu\text{m}^2$ in NE-0 to $3100 \pm 229 \mu\text{m}^2$ in NE-80, and the number of NPCs increased from 4400 ± 651 to 15800 ± 1054 NPCs (Fig.

Salk Institute for Biological Studies, Molecular and Cell Biology Laboratory, 10010 North Torrey Pines Road, La Jolla, CA 92037, USA.

*These authors contributed equally to this work
†To whom correspondence should be addressed. E-mail: hetzert@salk.edu

Fig. 1. Transport-independent role of Importin β in NPC insertion. **(A)** Nuclei (NE-0) were preassembled in 5- μl reactions including egg extracts, membranes, and sperm chromatin for 40 min (17), and diluted with 50 μl fresh cytosol in the absence or presence of 5 μM RanT24N, 2 mM GTP γ S, WGA (20 $\mu\text{g/ml}$), 2 μM transportin (Trn), or Importin β (Imp β) ($\pm 10 \mu\text{M}$ RanGTP), for an additional 80 min (NE-80) and analyzed by confocal microscopy. The formation of a closed NE was analyzed in unfixed nuclei using the membrane stain DilC₁₆ (1,1'-dihexadecyl-3,3,3',3'-tetramethylindocarbocyanine perchlorate) (27) and 70-kD dextran (small insert). Individual NPCs were visualized by immunofluorescence with mAb414 on the surface of the nuclei at low magnification (middle row) and with 8 \times zoom (bottom row). Scale bars, 10 μm .



(B) NE surface area and total number of pores were calculated using five independent experiments as described in (28). The relative increase of surface area (black) and pore numbers (gray) during 80 min were plotted.

Error bars indicate SD. **(C)** Nuclei were assembled in the absence (buffer) and presence of 2 μM Importin β , sectioned, and analyzed by transmission electron microscopy (17). Scale bar, 200 nm. Cyto, cytosol.

Fig. 2. RanGTP-mediated incorporation of Nup107-160 complex occurs from the nucleoplasmic and cytoplasmic side of the NE. (A) Fluorescently labeled RanT24N accumulated in assembled nuclei and was trapped in the nucleoplasm of WGA-sealed nuclei after dilution (T24N ⇒ WGA). RanT24N was excluded from the nucleoplasm when added after the NPCs were blocked with WGA (WGA ⇒ T24N). Scale bar, 10 μm. (B) The area labeled “control” shows the quantification of total pore numbers of NE-0 and NE-80 nuclei. The area labeled “T24N” shows data for NE-0 nuclei that were incubated with 5 μM RanT24N for 10 min. NPC insertion was induced with 200 volumes of cytosol (cyto) or 5 μM RCC1. To trap RanT24N inside the nucleus, NPCs were sealed with WGA (20 μg/ml) for 10 min, and NPC insertion was then induced by adding cytosol (WGA ⇒ cyto) or 5 μM RanGTP (WGA ⇒ RanQ69L). The area labeled “WGA” shows data for NE-0 nuclei that were incubated with WGA (20 μg/ml) for 10 min before the addition of cytosol (cyto), cytosol that contained 5 μM RanT24N (cyto[T24N]), or RanT24N and RanQ69L (cyto[T24N] ⇒ Q69L). The number of NPCs was quantified as described in Fig. 1. (C) NE-0 nuclei were incubated in the absence or presence of 5 μM RanGAP-RanBP1 or RanGAP-RanBP1 plus 5 μM RCC1 as indicated. Nuclei were stained with mAb414 (green) and DiI₁₆ (red) and analyzed in cross sections or (D) on the NE surface to visualize individual NPCs. Scale bars, 10 μm.

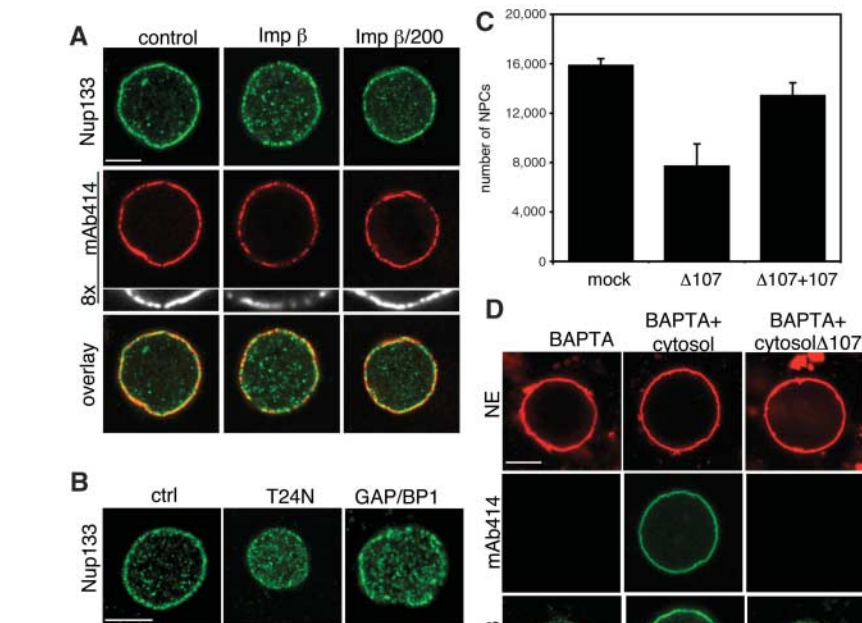
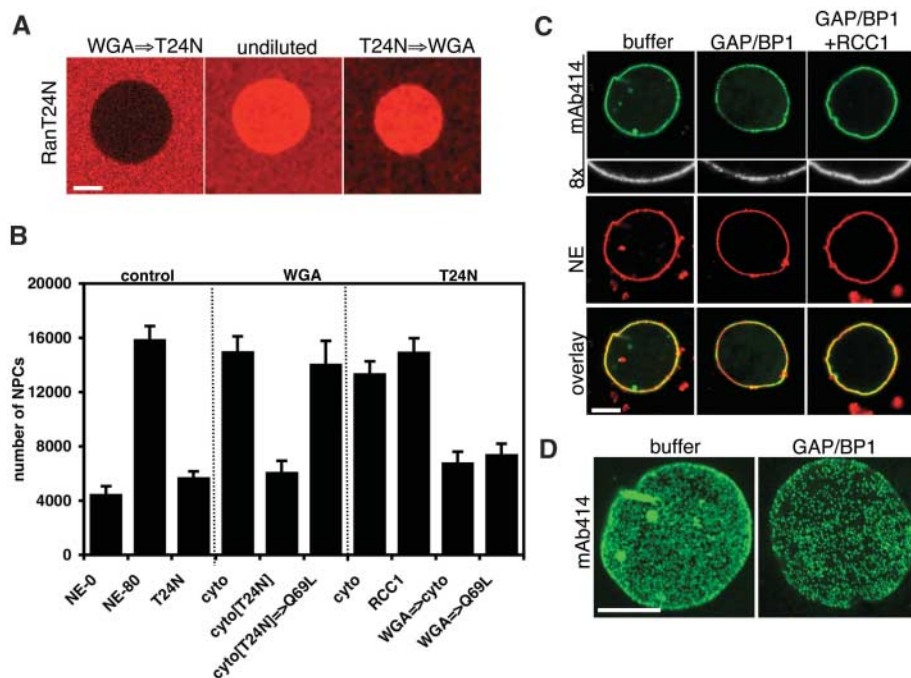


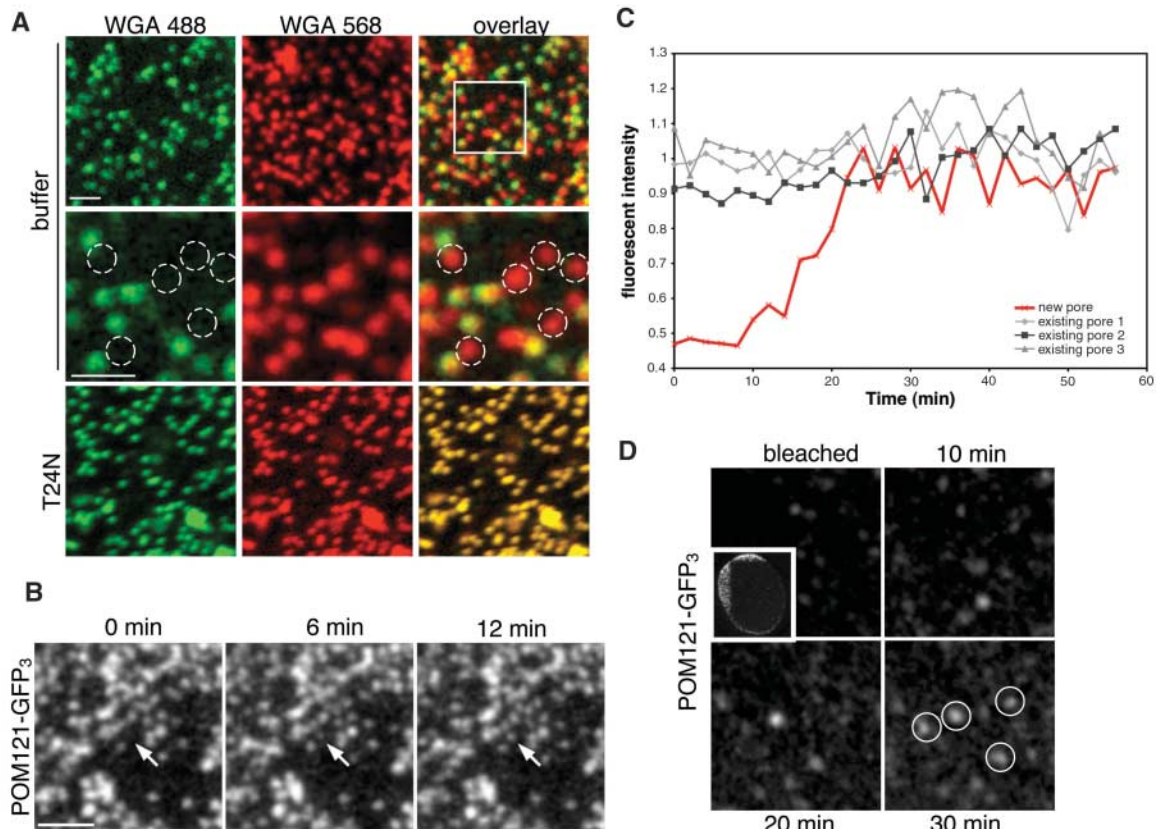
Fig. 3. Nucleoplasmic and cytoplasmic Nup107-160 complexes are required for NPC insertion. (A) NE-0 nuclei were incubated in 5 μl fresh cytosol to which buffer or 2 μM Importin β had been added, and nuclei were analyzed after 80 min by immunofluorescence using αNup133 and mAb414. To reverse the inhibitory effect of Importin β, NE-80 nuclei were diluted in 200 volumes of cytosol. Scale bar, 10 μm. (B) Nuclei were assembled in the presence of Importin β, and subsequently diluted in 200 volumes of cytosol (buffer), cytosol containing 5 μM RanT24N, or 10 μM RanGAP-RanBP1 for 30 min. Nuclei were analyzed by immunofluorescence using αNup133. Scale bar, 10 μm. (C) NE-0 nuclei were incubated at room temperature with mock-depleted or Nup107-160-depleted cytosol (in the absence or presence of purified Nup107-160 complex), and the total number of NPCs was quantified as in Fig. 1. Error bars indicate SD. (D) Nuclear assembly was performed using DiI₁₆-labeled NE membranes, sperm chromatin, and cytosol in the presence of 5 mM BAPTA for 60 min, and the nuclei were diluted with mock-depleted cytosol or Nup107-160-depleted cytosol. NPCs were visualized with mAb414 and αNup133. Scale bar, 10 μm.

1, A and B). NPC insertion occurred steadily at a rate of 142 ± 11 NPCs/min.

The insertion of new pores into intact nuclei occurs in the presence of nucleo-cytoplasmic transport, which is driven by the small guanosine triphosphatase (GTPase) Ran (2, 13). To test whether Ran-mediated transport was required for pore formation, we incubated NE-0 nuclei with cytosol in presence of RanT24N, a Ran mutant (where Thr²⁴ is replaced by Asn) that blocks the generation of RanGTP (14). NPC insertion, NE expansion (Fig. 1, A and B), and Ran-mediated nuclear transport (fig. S1D) were all strongly inhibited. The addition of two transport inhibitors—a nonhydrolyzable GTP analog (GTPγS) and wheat germ agglutinin (WGA), which blocks pores by binding to nucleoporins that contain *N*-acetylglucosamine residues (12, 15)—both inhibited nuclear import of bovine serum albumin–nuclear localization signal (BSA-NLS) (fig. S1D) and NE expansion (Fig. 1B). However, new NPCs were still efficiently inserted (Fig. 1, A and B), and the NPC density increased from 4.9 ± 0.6 to 10.3 ± 1.4 NPCs/μm² in the presence of GTPγS and to 8.3 ± 0.5 NPCs/μm² in the presence of WGA (Fig. 1, A and B). Thus, NPC insertion in vitro requires RanGTP but can occur in the absence of the nuclear transport activity of existing pores and NE expansion.

NPC assembly into the reforming NE at the end of mitosis is negatively regulated by the nuclear transport receptor Importin β (16, 17). We wanted to test Importin β's effect on new NPC insertion. In the presence of 2 μM Importin β, neither NE expansion (Fig. 1, A and B) nor nuclear import of BSA-NLS (fig. S1D)

Fig. 4. NPC insertion occurs by a de novo mechanism. **(A)** NE-0 nuclei were labeled with fluorescently labeled WGA-488 (10 $\mu\text{g/ml}$) for 10 min and subsequently incubated with 400 volumes of cytosol in the absence or presence of 5 μM RanT24N for 30 min. Fluorescently labeled WGA-568 was added for 10 min, and nuclei were analyzed by confocal microscopy. Newly formed pores are visible as red dots; they do not contain a detectable green signal. Scale bar, 1 μm . **(B)** HeLa cells expressing POM121-(GFP₃) were analyzed in real time by confocal microscopy on the NE surface every 2 min. Arrows indicate new NPC assembly site. **(C)** Relative fluorescence intensity of preexisting pores (gray) and new pores (red) was plotted against time. **(D)** Large areas of NEs were photobleached (inset), and the formation of few pores was monitored by 4D confocal microscopy. Bleached POM121-(GFP₃) did not recover for more than 4 hours, similar to previously published report (29).



were affected. However, NPC insertion was strongly inhibited when compared with control reactions containing transportin, an import receptor not involved in NPC assembly (Fig. 1, A and B) (17). The pore density dropped from 4.9 ± 0.6 NPCs/ μm^2 in control reactions to 2.2 ± 0.4 NPCs/ μm^2 in the presence of Importin β , an effect that was restored by 10 μM RanGTP (Fig. 1, A and B). Thus, Importin β negatively regulates NPC insertion into intact nuclei in a transport-independent manner.

To analyze from which sides of the NE nucleoporins were inserted, RanGTP production had to be blocked only in the cytoplasm or only in the nucleoplasm. First, NE-0 nuclei were assembled, and the existing pores were sealed with WGA at a concentration of 20 $\mu\text{g/ml}$ before adding either cytosol or cytosol-containing 5 μM RanT24N. RanT24N inhibited NPC insertion (Fig. 2B), even though it was excluded from the nucleus (Fig. 2A). NPC assembly was restored by the addition of 5 μM RanQ69L (where Gln⁶⁹ is replaced by Leu), a GTPase-deficient mutant of Ran (18, 19), or by 5 μM Ran's nucleotide exchange factor RCC1 (Fig. 2B), demonstrating that RanT24N specifically inhibited endogenous cytoplasmic RCC1.

Second, we added recombinant RanGAP-RanBP1 complex [Ran's GTPase activating protein (GAP) and its co-factor RanBP1 (14)], which are excluded from the nucleus (20) to

deplete cytoplasmic RanGTP. NPC insertion was blocked, but unlike the case with RanT24N, neither nuclear transport (fig. S1D) nor NE expansion were affected (Fig. 2C), and consequently, the pore density decreased (Fig. 2D). Thus, RanGTP, as previously suggested [see discussion in (21)], plays a cytoplasmic role in NPC insertion in vitro.

To inhibit nuclear RCC1, we incubated NE-0 nuclei with RanT24N, which accumulated in the nucleoplasm (Fig. 2A) and inhibited NPC insertion (Fig. 2B). After 10 min, either buffer or WGA was added to the reactions to seal the pores. When the WGA-treated nuclei were incubated with 200 volumes of fresh cytosol, RanT24N in the cytosol was diluted to noninhibitory levels. The concentration of RanT24N trapped inside the nucleus was unaffected (Fig. 2A), and NPC insertion was not restored (Fig. 2B). In contrast, nuclei that were diluted in the absence of WGA efficiently inserted new NPCs (Fig. 2B). Thus, the generation of RanGTP inside the nucleus is required for NPC insertion. Taken together, these results suggest that NPC assembly in egg extracts involves Ran-dependent steps on both sides of the NE. Whether somatic cells, which do not appear to have cytoplasmic RCC1 and RanGTP, use a different NPC insertion mechanism remains to be analyzed.

Our results imply a model in which RanGTP-mediated release of nucleoporins from Importin

β (17) occurs in both the nucleoplasmic and cytoplasmic compartment. To test whether soluble Importin β -binding nucleoporins, such as the Nup107-160 complex (17), are indeed present in both compartments, we stained NE-80 nuclei with antibodies against several nucleoporins (Fig. 3A and fig. S2). We detected a strong NE rim staining for all of them and an additional nucleoplasmic signal specifically with antibodies to Nup133 and Nup160, two components of the Nup107-160 complex, which has been shown to be essential for NPC formation (Fig. 3A) (22, 23). When the assembly of new pores into NE-0 nuclei was blocked by adding Importin β , an increase in nucleoplasmic Nup107-160 signal was observed, whereas the rim signal was reduced (Fig. 3A and fig. S2A). Diluting the nuclei with 200 volumes of fresh cytosol or the addition of RanGTP (24) reversed this effect, even when nuclear transport was blocked by WGA (Fig. 3B and fig. S2B). Similarly, the nucleoplasmic Nup107-160 signal increased when NPC insertion was blocked with RanT24N or RanGAP-RanBP1 (Fig. 2B), suggesting that the nucleoplasmic pool of Nup107-160, which is essential for pore formation (23), was not incorporated into the NE when RanGTP production was blocked.

Next we analyzed whether Nup107-160 complexes were incorporated from the cytoplasmic side of the NE. We assembled NE-0

nuclei and subsequently added WGA to seal the existing pores. A nucleoplasmic signal was detectable when these nuclei were stained with α Nup133 and α Nup160 (24). In contrast to mock-depleted cytosol, Nup107-160-depleted cytosol did not induce the assembly of new pores (Fig. 3C). This lack of activity was caused by the absence of Nup107-160, because the addition of purified Nup107-160 complex (fig. S2C) restored NPC insertion (Fig. 3C).

Nuclei were formed in the presence of BAPTA (1,2-bis(2-aminophenoxy)ethane- N,N,N',N' -tetraacetic acid), a calcium chelator that inhibits NPC formation (25), and a strong nucleoplasmic Nup133 signal was detected (Fig. 3D). When the BAPTA nuclei were diluted in mock-depleted cytosol, NPC insertion was restored, whereas Nup107-160-depleted cytosol failed to do so (Fig. 3D). Consistent with the cytoplasmic RanGTP-mediated release of Importin β from the Nup107-160 complex, we found that the addition of 5 μ M RanT24N resulted in a 60% increase of Importin β associated with immunoprecipitated Nup107-160 complex (24). Thus, the incorporation of the Nup107-160 complex into new assembly sites occurs from both sides of the NE. Because nuclear transport is not required for NPC insertion *in vitro*, the nucleoplasmic pool of Nup107-160 complexes might be generated via chromatin association during nuclear assembly (17).

Next we wanted to analyze if pores assemble *de novo* or by the splitting of existing pores (7–9). We assembled NE-0 nuclei and subsequently fluorescently labeled individual pores with WGA-488 (green) (Fig. 4A). Upon dilution, WGA-488 remained stably bound to NPCs while new unlabeled pores were inserted (fig. S3A), which could be labeled with WGA-568 (red). Newly formed pores were only labeled with WGA-568 and appeared as red dots, whereas old pores were labeled with both dyes resulting in a yellow overlay. The new pores did not exhibit green signal from existing pores, suggesting that NPCs form *de novo* (Fig. 4A). When the formation of new pores was blocked by the addition of 5 μ M RanT24N, all pores appeared yellow in the overlay (Fig. 4A), indicating that red dots represented newly formed pores. Furthermore, the average fluorescence intensity of WGA-488-labeled NPCs remained constant after dilution of the dye, and it was indistinguishable between nuclei that inserted new pores and nuclei where the formation of new NPCs was blocked by 5 μ M RanT24N (fig. S3B). These results suggest that newly formed pores do not incorporate nucleoporins from existing NPCs, and they support a *de novo* mechanism, because in a splitting process, the intensity of the old pores would be expected to decrease. Additionally, we were able to detect pores that stained with α POM121, a transmembrane nucleoporin, and Nup133,

but not with mAb414 (fig. S3C). POM121 colocalized with mAb414 when the formation of new NPCs was blocked by RanT24N (fig. S3C). This indicates that phenyl-glycyl-repeat nucleoporins are recruited to new assembly sites after POM121 and Nup107-160 complexes have been incorporated and further supports *de novo* formation.

To determine whether NPC formation *in vivo* also occurs by a *de novo* mechanism, we generated a stable HeLa cell line expressing low, nontoxic levels of POM121 containing multiple copies of green fluorescent protein (GFP) to visualize individual NPCs in living cells (26). Four-dimensional confocal time-lapse microscopy was used to follow NPC assembly during interphase and new pores became visible as single dots in areas where initially no GFP signal was detectable (Fig. 4B and Movie S1) and in areas where preexisting pores have been photobleached (Fig. 4D). New NPCs colocalized with neighboring, preexisting pores along the z axis (fig. S4, A and B), showing that they were inserted into the NE. Consistent with *de novo* formation, existing pores did not change fluorescence intensity over time (Fig. 4C). These findings further support a *de novo* mechanism for NPC biogenesis.

References and Notes

1. S. R. Wentz, *Science* **288**, 1374 (2000).
2. D. Gorlich, U. Kutay, *Annu. Rev. Cell Dev. Biol.* **15**, 607 (1999).
3. G. G. Maul, L. L. Deaven, J. J. Freed, G. L. Campbell, W. Becak, *Cytogenet. Cell Genet.* **26**, 175 (1980).
4. G. G. Maul *et al.*, *J. Cell Biol.* **55**, 433 (1972).
5. M. Winey, D. Yarar, T. H. Giddings Jr., D. N. Mastrorade, *Mol. Biol. Cell* **8**, 2119 (1997).
6. B. Burke, J. Ellenberg, *Nat. Rev. Mol. Cell Biol.* **3**, 487 (2002).
7. M. Hetzer, T. C. Walther, I. W. Mattaj, *Annu. Rev. Cell Dev. Biol.* (2005).

8. K. Bodoor *et al.*, *Biochem. Cell Biol.* **77**, 321 (1999).
9. G. Rabut, P. Lenart, J. Ellenberg, *Curr. Opin. Cell Biol.* **16**, 314 (2004).
10. M. J. Lohka, Y. Masui, *Science* **220**, 719 (1983).
11. M. Hetzer, D. Bilbao-Cortes, T. C. Walther, O. J. Gruss, I. W. Mattaj, *Mol. Cell* **5**, 1013 (2000).
12. L. I. Davis, G. Blobel, *Proc. Natl. Acad. Sci. U.S.A.* **84**, 7552 (1987).
13. M. Dasso, *Curr. Biol.* **12**, R502 (2002).
14. C. Klebe, H. Prinz, A. Wittinghofer, R. S. Goody, *Biochemistry* **34**, 12543 (1995).
15. D. R. Finlay, E. Meier, P. Bradley, J. Horecka, D. J. Forbes, *J. Cell Biol.* **114**, 169 (1991).
16. A. Harel *et al.*, *Mol. Biol. Cell* **14**, 4387 (2003).
17. T. C. Walther *et al.*, *Nature* **424**, 689 (2003).
18. F. R. Bischoff, C. Klebe, J. Kretschmer, A. Wittinghofer, H. Ponstingl, *Proc. Natl. Acad. Sci. U.S.A.* **91**, 2587 (1994).
19. C. Klebe, F. R. Bischoff, H. Ponstingl, A. Wittinghofer, *Biochemistry* **34**, 639 (1995).
20. D. Gorlich, *Curr. Opin. Cell Biol.* **9**, 412 (1997).
21. K. J. Ryan, J. M. McCaffery, S. R. Wentz, *J. Cell Biol.* **160**, 1041 (2003).
22. A. Harel *et al.*, *Mol. Cell* **11**, 853 (2003).
23. T. C. Walther *et al.*, *Cell* **113**, 195 (2003).
24. M. A. D'Angelo, D. J. Anderson, E. Richard, M. W. Hetzer, data not shown.
25. C. Macaulay, D. J. Forbes, *J. Cell Biol.* **132**, 5 (1996).
26. N. Daigle *et al.*, *J. Cell Biol.* **154**, 71 (2001).
27. M. Hetzer *et al.*, *Nat. Cell Biol.* **3**, 1086 (2001).
28. Materials and methods are available as supporting material on Science Online.
29. G. Rabut, V. Doye, J. Ellenberg, *Nat. Cell Biol.* **6**, 1114 (2004).
30. Antibodies against Importin β were kindly provided by L. Gerace. We thank the members of our laboratory and T. Hunter for helpful discussions and W. Eckhart, J. Karlseder, V. Lundblad, J. Young, B. Sefton, and M. Weitzman for critically reading the manuscript. M.A.D. and M.H. were supported by The Pew Charitable Trust.

Supporting Online Material

www.sciencemag.org/cgi/content/full/312/5772/440/DC1
Materials and Methods
Figs. S1 to S4
Movie S1

22 December 2005; accepted 14 March 2006
10.1126/science.1124196

Differential Targeting of G $\beta\gamma$ -Subunit Signaling with Small Molecules

Tabetha M. Bonacci,¹ Jennifer L. Mathews,¹ Chujun Yuan,² David M. Lehmann,¹ Sundeep Malik,¹ Dianqing Wu,³ Jose L. Font,¹ Jean M. Bidlack,¹ Alan V. Smrcka^{1,2*}

G protein $\beta\gamma$ subunits have potential as a target for therapeutic treatment of a number of diseases. We performed virtual docking of a small-molecule library to a site on G $\beta\gamma$ subunits that mediates protein interactions. We hypothesized that differential targeting of this surface could allow for selective modulation of G $\beta\gamma$ subunit functions. Several compounds bound to G $\beta\gamma$ subunits with affinities from 0.1 to 60 μ M and selectively modulated functional G $\beta\gamma$ -protein-protein interactions *in vitro*, chemotactic peptide signaling pathways in HL-60 leukocytes, and opioid receptor-dependent analgesia *in vivo*. These data demonstrate an approach for modulation of G protein-coupled receptor signaling that may represent an important therapeutic strategy.

The $\beta\gamma$ subunits of heterotrimeric guanine nucleotide binding proteins (G proteins) are released upon ligand activation of G protein-coupled receptors (GPCRs). Free G $\beta\gamma$ subunits bind and regulate multiple target

proteins within the cell—including phospholipase C (PLC) β 2 and PLC β 3, phosphoinositide 3 kinase (PI3K) γ , adenylyl cyclase, N-type Ca²⁺ channels, and inwardly rectifying K⁺ channels—and mediate physiological